

Investigation of Structural Plate with Cracks and Hole under Combined Loading

Markad Kanif M¹, Khubi Lal Khatri² and Vaghela Manoj B³

¹Department of Mechanical Engineering, DVVP College of Engineering, Ahmednagar, Maharashtra, India

²Department of Mechanical Engineering, Swarnim institute of Technology, Gandhinagar, Gujarat, India

³Department of Mechanical Engineering, Lukhdhirji Engineering College, Morbi, Gujarat, India

Abstract. Here, XFEM is used to model structural discontinuities like cracks and holes in order to forecast the strength and dependability of the structure under service conditions. By contrasting the numerical outcomes of several issues with the analytical and experimental findings, the method's resilience has been shown. Additionally, XFEM is coupled with a stochastic method to predict the sensitivity of a structure with discontinuities (cracks and holes) under tensile loading conditions in terms of output COVs and fracture strength in terms of mean values of stress intensity factors (SIFs) using input individual and combined randomness in various system parameters. The second order perturbation technique has been utilized in stochastic / perturbation theory to forecast how constructions would fracture. The perturbation technique is also utilized as Taylor series expansion method and yields accurate results if the input randomness is less than twenty percentage.

Keywords. XFEM, COV, MMSIF, Stochastic, Perturbation

1. Introduction

We are aware that randomness always exists in reality and affects every aspect of a construction, including its geometry, strength, lifespan, susceptibility to damage, and fracture parameters. Even with the finest quality control procedures, randomness in system attributes has a major impact on how the mechanical

component responds to fracture. Therefore, randomness, external loads, material qualities, crack parameters, and geometry must all be taken into account when performing a fracture analysis on a structure. The stochastic fracture analysis increases the safety of structures by offering a reliable prediction of the fracture behaviour of the structure. The reliability evaluation methodologies can aid in the creation of preliminary recommendations for reliable designs. Many scholars have successfully analysed the stochastic fracture behaviour of the structure. Through the use of several numerical examples and the scaled boundary finite element method (SBFEM), Chowdhury et al. [1] completed the shape sensitivity analysis (Rahman and Chen [2]; Reddy and Rao [3]) of stress intensity variables to the crack size and direction. They performed the reliability assessment by Monte Carlo simulations (Chakraborty and Rahman [4, 5]; Choi et al. [6]; Evangelatos and Spanos [7]; Haldar and Mahadevan [8]; Khasin [9]; Lal and Palekar [10]). Some academics have talked about their work using the perturbation technique to forecast the material's stochastic reaction. In this regard, Rahman and Rao [11] introduced a stochastic meshless technique for resolving random material property boundary-value issues in linear elasticity. For the purpose of forecasting stochastic structure response, they created a meshless formulation. Classical perturbation expansions were produced in conjunction with the meshless equations to forecast the response's second-moment characteristics.

The XFEM has been further improved or enhanced by many researchers through coupling the XFEM with another technique to overcome the difficulties faced by the general XFEM. In the direction, a new set of enrichment functions was proposed for solving the Poisson equation in 1D and 2D spaces and was reduced the analysis error by Paweł [12]. The XFEM was coupled with a constitutive law with embedded discontinuity (CLED) approach for modelling of mixed mode cracking in concrete structure for simplifying the numerical implementation (Pietruszczak and Haghghat, [13]). Improved XFEM was developed for 3D and demonstrated better accuracy, convergence and efficiency. It overcomes the linear dependency problem by utilizing an extra degree of freedom free partition of unity approximation which is based on local least-squares fitting with a one-point interpolation constraint (Tian et al., [14]).

Using XFEM and various independent, combined uncorrelated and correlated input random Gaussian variables using SOPT and MCS, Lal and Markad [15] presented mixed mode SIFs and crack propagation analysis of the symmetric angle-ply laminated composite plate with through-thickness arbitrary curve cracks subjected to tensile and shear stress. The stochastic finite element technique is an extension of the MCS with uncertainty in the system parameters, such as materials, geometry, etc. given by Arregui-Mena et al. [16]. The spectral stochastic finite element approach and the perturbation technique (SSFEM). Lal and Markad [10] utilised a C^0 FEM based on higher order shear deformation plate theory was used to evaluate the second order statistics of MMSIFs of single edge V-notched angle-ply laminated composite plates under in-plane tensile load with uncertainty in material parameters, crack opening, and fracture length (HSDT). With the help of FOPT, SOPT, and MCS, the probabilistic evaluation was carried out.

The few researchers predicted how an infinite plate with a separate circular hole and a crack would fracture under tensile force. To the author's knowledge, XFEM with SOPT has not been used to investigate the stochastic fracture behaviour in terms of normalised MMSIFs and corresponding COVs of the infinite plate with various positions of a separate circular hole and a crack with various crack angles under tensile loading with input random parameters such as crack length, normalised radius of the hole, crack angle, and the central distance between separate hole and crack.

By incorporating the individual and combined randomness in the normalised crack length, crack angle, and normalised radius of the hole in an isotropic plate with a hole emanating cracks using SOPT, the stochastic fracture response through the normalised MMSIFs is calculated. Some results are validated with MCS. Present work is also focused on effect of combined loading over stochastic fracture response of the structural plate in terms of normalized MMSIFs.

2. Mathematical formulation

The XFEM is useful for modelling discontinuities like fractures, holes or voids, inclusions, interfaces, etc. while including discontinuous functions in the FE mesh. The level set method (LSM) has been successfully

used in conjunction with the XFEM to address these problems by providing further enrichment functions like crack faces and crack tips. Here, the XFEM software is built upon the 2D MATLAB code by Pais [18].

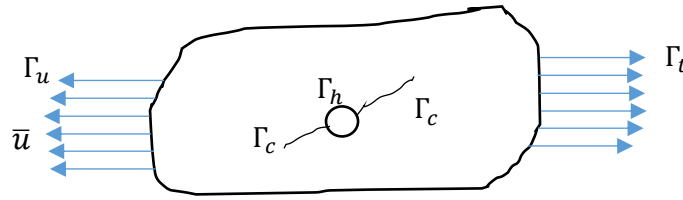


Fig. 1 Area under consideration with cracks, holes, and boundary condition

2.1 Equilibrium equation

The surfaces of cracks Γ_c and holes Γ_h are assumed traction free as are mentioned by Daux et al. [20], and shown in figure 1. The equilibrium equation in the domain Ω is:

$$\tilde{\nabla} \cdot \boldsymbol{\sigma}_t + \mathbf{f}_b = 0 \quad (1)$$

Small strains and displacements are taken into consideration in the current work. Thus, the relationship between strain and displacement illustrates the kinematics equations:

$$\boldsymbol{\varepsilon} = \boldsymbol{\varepsilon}(\mathbf{u}) = \tilde{\nabla}_s \cdot \mathbf{u} \quad (2)$$

Here, $\tilde{\nabla}_s$ is the symmetric part of the gradient operator and \mathbf{u} is a displacement field vector. The boundary conditions for the displacements on the boundary Γ_u are:

$$\mathbf{u} = \bar{\mathbf{u}}. \quad (3)$$

The constitutive relation for elastic material can be shown by Hooke's law as:

$$\boldsymbol{\sigma}_t = \mathbf{D} \cdot \boldsymbol{\varepsilon}(\mathbf{u}) \quad (4)$$

where \mathbf{D} is Hooke tensor or constitutive matrix for isotropic materials for plane stress and strain conditions in 2D.

The equilibrium equations' weak form is provided by:

$$\int_{\Omega} \boldsymbol{\varepsilon}(\mathbf{u}) : \mathbf{D} : \boldsymbol{\varepsilon}(\mathbf{v}) d\Omega = \int_{\Omega} \bar{\mathbf{b}} \cdot \mathbf{v} d\Omega + \int_{\Gamma_t} \bar{\mathbf{t}} \cdot \mathbf{v} d\Gamma \quad \forall \mathbf{v} \in \gamma_0 \quad (5)$$

The linear, FF and bilinear, SS forms of the equation (5) are:

$$FF(\mathbf{v}) = \int_{\Gamma} \bar{\mathbf{b}} \cdot \mathbf{v} d\Omega + \int_{\Gamma_r} \bar{\mathbf{t}} \cdot \mathbf{v} d\Omega \quad (6)$$

$$SS(\mathbf{u}, \mathbf{v}) = \int_{\Omega} \boldsymbol{\varepsilon}(\mathbf{u}) : \mathbf{D} : \boldsymbol{\varepsilon}(\mathbf{v}) d\Omega \quad (7)$$

$$\text{Potential energy } (\Pi) \text{ of an elastic body is } \Pi = \frac{1}{2} SS(\mathbf{u}, \mathbf{u}) - FF(\mathbf{u}) \quad (8)$$

By applying a variant of the previous equation and substituting $\frac{\partial \Pi}{\partial \mathbf{u}} = 0$, the minimization of the elastic

body's potential energy may be solved, and the following set of discrete equations is produced as a result.

$$[\mathbf{K}]\{\mathbf{d}\} = \{\mathbf{f}\} \quad (9)$$

where, $[\mathbf{K}]$ is the global stiffness matrix, $\{\mathbf{d}\}$ are the global degrees of freedom and $\{\mathbf{f}\}$ are the applied loading or force.

$$\mathbf{K}_{ij}^e = \begin{bmatrix} \mathbf{K}_{ij}^{uu} & \mathbf{K}_{ij}^{ua} & \mathbf{K}_{ij}^{ub} & \mathbf{K}_{ij}^{ug} \\ \mathbf{K}_{ij}^{au} & \mathbf{K}_{ij}^{aa} & \mathbf{K}_{ij}^{ab} & \mathbf{K}_{ij}^{ag} \\ \mathbf{K}_{ij}^{bu} & \mathbf{K}_{ij}^{ba} & \mathbf{K}_{ij}^{bb} & \mathbf{K}_{ij}^{bg} \\ \mathbf{K}_{ij}^{gu} & \mathbf{K}_{ij}^{ga} & \mathbf{K}_{ij}^{gb} & \mathbf{K}_{ij}^{gg} \end{bmatrix} \quad (10)$$

$$\mathbf{f}_i^e = \{\mathbf{f}_i^u \quad \mathbf{f}_i^a \quad \mathbf{f}_i^{b_1} \quad \mathbf{f}_i^{b_2} \quad \mathbf{f}_i^{b_3} \quad \mathbf{f}_i^{b_4} \quad \mathbf{f}_i^g\}^T \quad (11)$$

$$\mathbf{d} = \{\mathbf{u} \quad \mathbf{a} \quad \mathbf{b}_1 \quad \mathbf{b}_1 \quad \mathbf{b}_1 \quad \mathbf{b}_1 \quad \mathbf{g}\}^T \quad (12)$$

2.2 XFEM Approximation

XFEM Approximation for Cracks and voids are defined as,

$$\mathbf{u}^h(\mathbf{x}) = \mathbf{u}^{\text{FEM}} + \mathbf{u}^{\text{ENR}} = \sum_{i=1}^n \mathcal{N}_i(\mathbf{x}) \left\{ \bar{\mathbf{u}}_i + \sum_{j=1}^m \mathbf{F}^j(\mathbf{x}) \mathbf{a}_i^j \right\} \quad (13)$$

Heaviside function for a discontinuous function for the crack and voids defined as,

$$\mathcal{H}_1(\mathbf{x}) = \begin{cases} 1 & \text{for } \varphi(\mathbf{x}) > 0 \\ 0 & \text{for } \varphi(\mathbf{x}) = 0 \\ -1 & \text{for } \varphi(\mathbf{x}) < 0 \end{cases} \quad \text{and} \quad \mathcal{H}_2(\mathbf{x}) = \begin{cases} 1 & \text{for } \chi(\mathbf{x}) > 0 \\ 0 & \text{for } \chi(\mathbf{x}) \leq 0 \end{cases} \quad (14)$$

2.3 Level Set Method

For crack, level set method implemented by eq. (15), and for voids by eq. (16). The sign distance function

$\phi(\mathbf{x}, t)$ to the curve Γ_c

$$\phi(\mathbf{x}) = \begin{cases} \min_{\mathbf{x}_c \in \Gamma} \|\mathbf{x} - \mathbf{x}_c\| = d(\mathbf{x}, \mathbf{x}_i) & \forall (\mathbf{x} - \mathbf{x}_c) \cdot \mathbf{e}_2 \geq 0 \\ \min_{\mathbf{x}_c \in \Gamma} \|\mathbf{x} - \mathbf{x}_c\| = -d(\mathbf{x}, \mathbf{x}_i) & \text{otherwise} \end{cases} \quad (15)$$

$$\chi(\mathbf{x}, 0) = \min_{\mathbf{x}_c^i \in \Omega_c^i} \left\{ \|\mathbf{x} - \mathbf{x}_c^i\| - r_c^i \right\} \quad \text{where, } i = 1, 2, \dots, n_c \quad (16)$$

where, d is the absolute distance, \mathbf{x}_i is the point on crack closest to a point \mathbf{x} with any point \mathbf{x}_c on the crack surface Γ_c . r_c^i is the radius of the i th hole.

2.4 Evaluation of Stress Intensity Factors (SIFs)

For general mixed-mode problems in two dimensions, SIFs and J-integral can be stated as,

$$J = \frac{K_I^2}{E^*} + \frac{K_{II}^2}{E^*} \quad (17)$$

$$\text{where, } E^* = \begin{cases} E & \text{for plane stress} \\ \frac{E}{1-\nu^2} & \text{for plane strain} \end{cases} \quad (18)$$

The J -integral also follows the path-independence and it is explained

$$J = \int_{\Gamma} \left(W n_j - \mathbf{t}_i \cdot \frac{\partial \mathbf{u}_i}{\partial x} \right) d\Gamma \quad (19)$$

where, W is the strain energy density. For the plate of the elastic material, it can explain that

$$W = (1/2) \boldsymbol{\sigma}_{ij} \boldsymbol{\varepsilon}_{ij} .$$

Now, two equilibrium, independent states of a cracked body are considered. Consider the state 1, $(\sigma_{ij}^{(1)}, \varepsilon_{ij}^{(1)}, \mathbf{u}_j^{(1)})$, corresponds to the present or actual state and state 2, $(\sigma_{ij}^{(2)}, \varepsilon_{ij}^{(2)}, \mathbf{u}_j^{(2)})$, is an auxiliary state. Further, $\sigma_{ij}^{(2)}$, $\varepsilon_{ij}^{(2)}$ and $\mathbf{u}_j^{(2)}$ are the auxiliary stress field, auxiliary strain field and auxiliary displacement field, respectively. Thus, superposition of these two states brings another equilibrium state, say, $(\sigma_{ij}, \varepsilon_{ij}, \mathbf{u}_j)$. Now, we have:

$$\sigma_{ij} = \sigma_{ij}^{(1)} + \sigma_{ij}^{(2)} \quad \varepsilon_{ij} = \varepsilon_{ij}^{(1)} + \varepsilon_{ij}^{(2)} \quad \mathbf{u}_j = \mathbf{u}_j^{(1)} + \mathbf{u}_j^{(2)} \quad (20)$$

The strain energy densities are:

$$W = W^{(1)} + W^{(2)} \quad W^{(1)} = \frac{1}{2} \sigma_{ij}^{(1)} \varepsilon_{ij}^{(1)} \quad W^{(2)} = \frac{1}{2} \sigma_{ij}^{(2)} \varepsilon_{ij}^{(2)} \quad (21)$$

$$W = \frac{1}{2} \sigma_{ij} \varepsilon_{ij} = \frac{1}{2} (\sigma_{ij}^{(1)} + \sigma_{ij}^{(2)}) (\varepsilon_{ij}^{(1)} + \varepsilon_{ij}^{(2)}) = \frac{1}{2} (W^{(1)} + W^{(2)}) - \sigma_{ij}^{(1)} \varepsilon_{ij}^{(2)} \quad (22)$$

2.5 Stress intensity factor (SIF)

The Mode-I and Mode-II SIFs are formulated as,

$$K_I = K_I^{(1)} + K_I^{(2)} \quad K_{II} = K_{II}^{(1)} + K_{II}^{(2)} \quad (23)$$

The Mode-I and Mode-II SIFs for the actual state can be obtained by choosing the auxiliary state (state 2), e.g., if auxiliary state 2 is chosen to be state for Mode-I, then the auxiliary state is Mode-I near tip displacement and stress field, then by putting $K_I^{(2)} = 1$ and $K_{II}^{(2)} = 0$ in the equation (23), we have:

$$K_I^{(1)} = \frac{M^{(1, \text{Mode I})} E^*}{2} \quad (24)$$

Similarly, if auxiliary state 2 is chosen to be state for Mode-II, then the auxiliary state is Mode-II near tip displacement and stress field, then by putting $K_I^{(2)} = 0$ and $K_{II}^{(2)} = 1$ in equation (23), we have:

$$K_{II}^{(1)} = \frac{M^{(1, \text{Mode II})} E^*}{2} \quad (25)$$

where, $M^{(1, \text{Mode I})}$ and $M^{(1, \text{Mode II})}$ are interaction integrals.

3. Results and discussion

By incorporating the individual and combined randomness in the normalised crack length ($e_1 = a/W$), crack angle ($e_2 = \alpha$), and normalised radius of the hole ($e_3 = R/W$) in an isotropic plate with a hole emanating cracks using SOPT, the stochastic fracture response through the normalised MMSIFs is calculated. Some results are validated with MCS. The input random variables are indicated by the parameter $\{e_i (i=1, 2 \text{ and } 3)\}$. Furthermore, it is assumed that the input COV for individual and combined randomness in all the parameters is 15% or 0.15 variation of characteristics from their mean values in order to forecast the stochastic MMSIFs of the plate under tensile, shear, and combination (tensile and shear) loadings. The percentage of the input random parameters has been randomly adopted because in perturbation technique, for input COVs < 0.2 or 20 %, the solution can be obtained up to the acceptable accuracy (Stefanou [20]).

The normalized MMSIFs in terms of K_I and K_{II} are expressed as:

For Tensile loading

$$K_I = K_{I, \text{mean}} / (\sigma \sqrt{\pi a}) \text{ and } K_{II} = K_{II, \text{mean}} / (\sigma \sqrt{\pi a}) \quad (26)$$

For Shear loading

$$K_I = K_{I, \text{mean}} / (\tau \sqrt{\pi a}) \text{ and } K_{II} = K_{II, \text{mean}} / (\tau \sqrt{\pi a}) \quad (27)$$

where $K_I, K_{II}, K_{I, \text{mean}}, K_{II, \text{mean}}, \sigma, \tau$ and λ are normalized Mode-I and Mode-II SIFs, numerical Mode-I and Mode-II SIFs, tensile, shear and combined stresses, respectively and where, $\lambda = \sigma = \tau$.

3.1 Convergence and validation study

The results of Grasa et al. [21] using a first-order perturbation technique (FOPT) on the basis of analytical and XFEM solution for an isotropic edge cracked plate subjected to tensile loading are available and are compared with the mean value of Mode-I SIF using the current perturbation-based SOPT combined with XFEM, and they are in good agreement as shown in Table 1.

Table 1 Validation of SIFs of an isotropic edge cracked plate subjected to tensile loading

Analytical Solution [21]	XFEM with FOPT [21]	% Error	XFEM with SOPT	% Error	XFEM with MCS	% Error
99.8182	98.951	0.87	100.4834	0.67	100.1276	0.31

Rarely are the SOPT findings for the stochastic fracture analysis of the investigated model under various stress situations available in the literature. To validate the current stochastic fracture analysis for $a/W=0.4$ with $\alpha=30^\circ$, as indicated in Table 2, the current mean and corresponding COV $\{e_i(i=1, 2 \text{ and } 3) = 0.15\}$ of MMSIFs K_I and K_{II} acquired by SOPT are compared with those obtained by MCS.

Table 2 Behaviour of the analyzed model under different loading conditions for normalized crack length ($a/W=0.4$) with crack angles ($\alpha=30^\circ$) through individual randomness in a/W by MCS with different numbers of samples

Total no. of samples	Tensile loading				Shear loading			
	K_I		K_{II}		K_I		K_{II}	
	Mean	COV	Mean	COV	Mean	COV	Mean	COV
9000	0.809	0.121	0.354	0.223	2.527	0.059	1.296	0.125
9500	0.822	0.084	0.342	0.197	2.536	0.051	1.193	0.097
10000	0.828	0.056	0.334	0.167	2.540	0.047	1.128	0.081
10500	0.828	0.056	0.334	0.167	2.540	0.047	1.128	0.081
11000	0.828	0.056	0.334	0.167	2.540	0.047	1.128	0.081

The results obtained by both SOPT and MCS are in very good agreement. In the direct MCS method, the different sets of random samples of random system properties are generated first by direct use of the computer by using Gaussian random number generation. These sets of random samples are substituted in the response equation of MMSIFs and again generated the random samples of MMSIFs. The mean of these random samples gives the mean value of MMSIFs, while the variance of random samples gives the variance of MMSIFs. The optimum numbers of samples are decided on the basis of convergence of mean results. In the present analysis, 10,000 samples are used for satisfactory convergence of the results. Therefore, the 10,000 random samples are used for further computation of results using MCS. In the present study, MCS is used only for validation purpose due to higher consumption of computational time, particularly for fracture problem with very high mesh density.

Fig. 2(a) and 2(b) show the line diagram of an isotropic rectangular plate with the analyzed model with dimensions of length ($2L$), width ($2W$), crack length ($2a$), and hole radius (R) and a central cracked plate without hole with required above-mentioned dimensions, under shear (τ) stress.

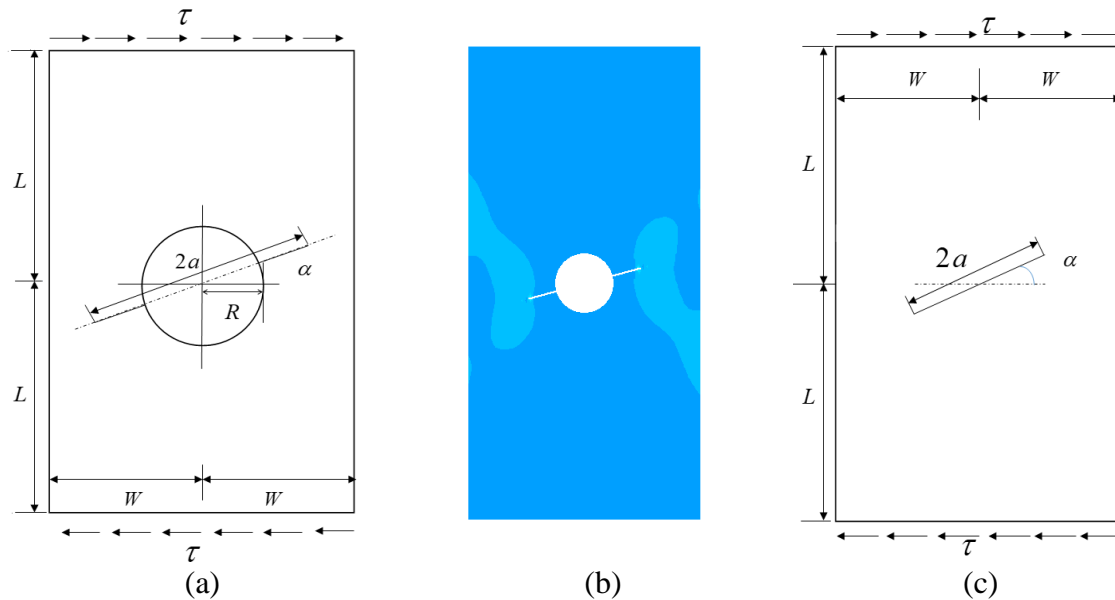


Fig. 2 (a) A line diagram and (b) the stress contour (general) of a plate with radial cracks on a hole and (c) a line diagram of central crack under shear loading

The behaviour of mean values of normalized MMSIFs of the analyzed model under uniform shear loading w.r.t. different crack angles is presented in Fig. 3(a) and 3(b). It is again clear that the SOPT results are in good agreement with those of MCS.

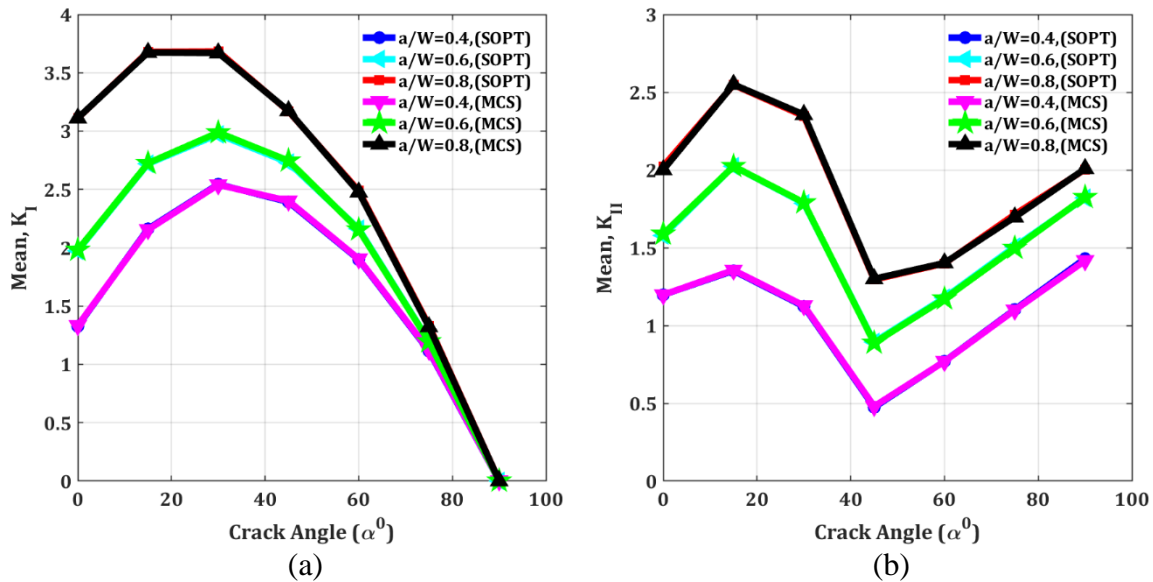


Fig. 3 The mean values of normalized MMSIFs (a) K_I and (b) K_{II} of a plate under shear loading with individual randomness in e_1 , e_2 and e_3

It can be seen that the mean values of K_I are largest at a crack angle $\alpha = 30^\circ$, and due to the increment in a/W , the mean values of K_I starts to dominate at $\alpha = 15^\circ$. As the crack angle (α) increases from 0° to 30° , the mean values of K_I are increased. Then, these values are continuously decreased to zero at 90° crack angle. Now, the mean values of normalized Mode-II SIFs K_{II} of the analyzed model are maximum at 15° crack angle and are minimum at 45° crack angle. At $\alpha = 0^\circ$ and 90° , the mean values of K_{II} are nearly equal as the normalized crack length increases ($a/W = 0.8$). From crack angle 45° to 90° , the mean values of K_I and K_{II} continuously decrease and increase, respectively.

Fig. 4(a) and 4(b) show the behaviour of the mean values of normalized MMSIFs K_I and K_{II} of the analyzed model under uniform tensile loading with individual randomness $\{e_i (i=1, 2 \text{ and } 3)\}$ with respect to different crack angles using SOPT and MCS.

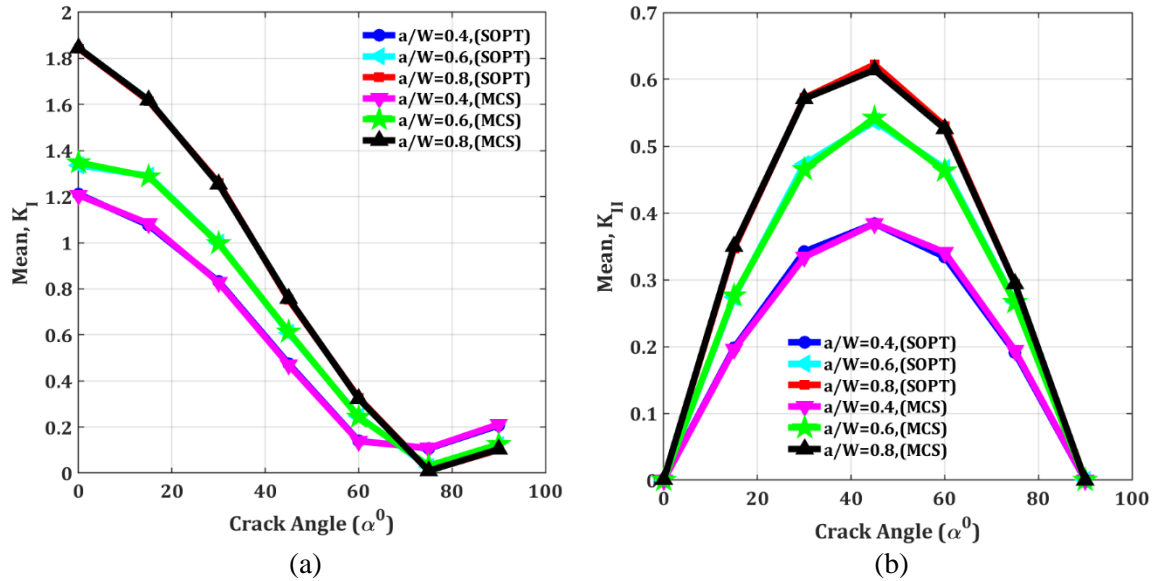


Fig. 4 The mean values of normalized MMSIFs (a) K_I and (b) K_{II} of plate under tensile loading with individual or combined randomness in e_1 , e_2 and e_3

It is clear that the SOPT results are in good agreement with those obtained using MCS. It can be seen that the mean values of normalized Mode-I SIFs K_I of the analyzed model are the largest at a crack angle $\alpha = 0^\circ$, and the SIFs K_I are decreased with increment in the crack angle till 75° . At 90° crack angle, the SIFs K_I for the shorter crack lengths a/W are further increased and it is so because the compressive stresses dominant and so the tips of longer crack will get less influence of the buckling, as compared to the shorter ones and the results is the higher SIFs in shorter cracks and the lower SIFs for longer cracks. The mean values of normalized Mode-II SIFs K_{II} of the analyzed model are largest at a crack angle $\alpha = 45^\circ$ and are minimum (zero) at $\alpha = 0^\circ$ and 90° . For the crack angles α and $(90^\circ - \alpha)$, the mean values of K_{II} are almost equal if the normalized crack length ($a/W = 0.4$ and 0.6) is shorter. For the longer cracks ($a/W = 0.8$), the mean values of K_{II} are not the same.

Fig. 5(a) and 5(b) show the line diagram of the analyzed model with dimensions of length ($2L$), width ($2W$), crack length ($2a$), and hole radius (R) and a central cracked plate without hole with required above-mentioned dimensions, under combined tensile (σ) and shear (τ) stresses.

The behaviour of the mean values of normalized MMSIFs K_I and K_{II} of the analyzed model w.r.t. different crack angles using SOPT is predicted and compared with the deterministic values of normalized MMSIFs K_I and K_{II} of the plate with a central crack without any hole with the same geometrical properties subjected to combined loading, as shown in Fig. 6(a) and 6(b).

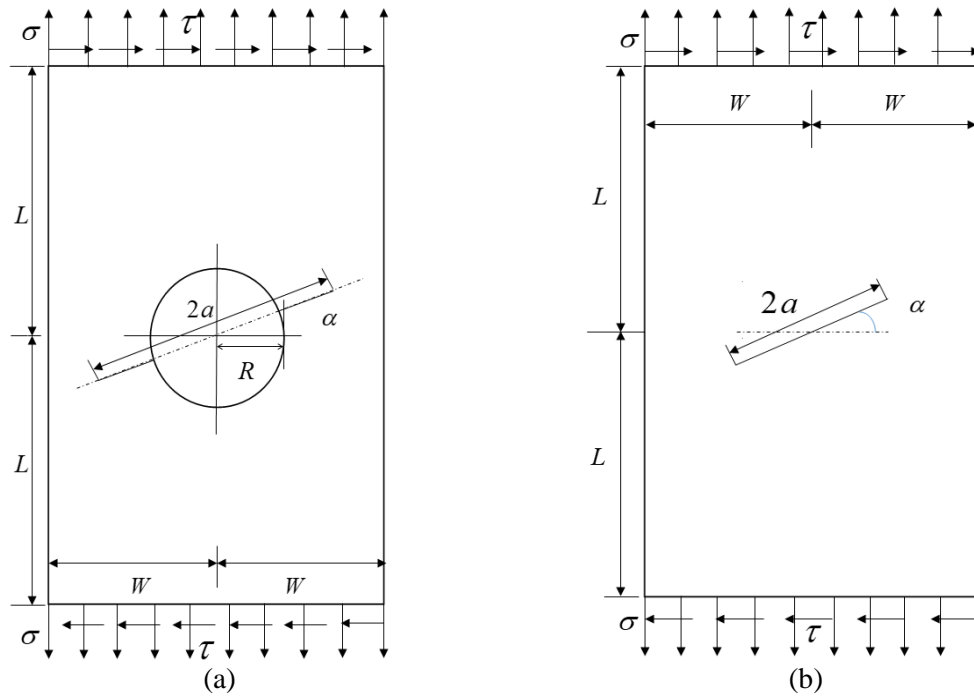


Fig. 5 Line diagrams of the plates with (a) hole emanating radial cracks and (b) a central crack subjected to combined loadings

It can be seen that the mean values of normalized Mode-I SIFs K_I are highest at crack angle $\alpha = 0^\circ$. Also, as the crack angle (α) is increased, the mean values of K_I are decreased from 0° to 90° crack angle. At 90° crack angle, the mean values of K_I are zero. For the crack angle 15° , the mean values of K_I are increased for shorter crack length ($a/W = 0.4$) because due to combined loading the stress concentration on the periphery of the hole, from where the cracks are emanating, will be maximum and the stress concentration zone will be upper and lower parts of the sides of the hole and crack. As the crack makes an angle of 30° , the tip of the crack will be much nearer to the stress concentration zone and more stresses will be on a crack tip, therefore, the mean values of K_I are continuously increased till angle 45° and remain

critical. After 45° angle, the crack tips gradually leave the stress concentration zone till angle 90° . But, for longer crack, the crack tip remains somewhat away from the periphery of the hole. That is why the stress concentration zone becomes unable to produce much effect on the crack tip. If the length of the emanating cracks is very large, then the hole becomes the part of crack only.

The mean values of normalized Mode-II SIFs K_{II} are highest at a crack angle $\alpha = 15^\circ$ but as a/W increases, the values of K_{II} start to dominate at $\alpha = 30^\circ$. From crack angles 30° to 60° and 60° to 90° , the mean values of K_{II} decreased and increased, respectively. Now, the mean values of normalized Mode-II SIFs K_{II} of an isotropic plate with a hole emanating radial cracks are the largest at 15° crack angle and are minimum at 60° crack angle.

At 90° crack angle, the mean value of K_I is zero because here, the effect of K_I is completely ineffective under the shear and combined loading. The mean values of normalized MMSIFs K_I and K_{II} of an isotropic plate with a hole emanating radial cracks subjected to combined and shear loadings are much higher as compared to those are under tensile loading. So, it can be concluded that the combined loading is much critical as compared to tensile and shear loading for the present problem.

Under all types of loading conditions, the gaps between the graphs, for the mean values of normalized MMSIFs K_I and K_{II} and the deterministic values of MMSIFs $K_{I,\text{det}}$ and $K_{II,\text{det}}$, are decreased as (a/W) is increased. It is so because the smaller crack with the hole has the influence on stress concentration as well as it works as a small edge crack on the periphery of the hole, whereas for the larger crack, the hole works as a part of the crack only or the role of the hole is just like a crack. Also, the mean values of normalized MMSIFs K_I and K_{II} are increased with increment in a/W .

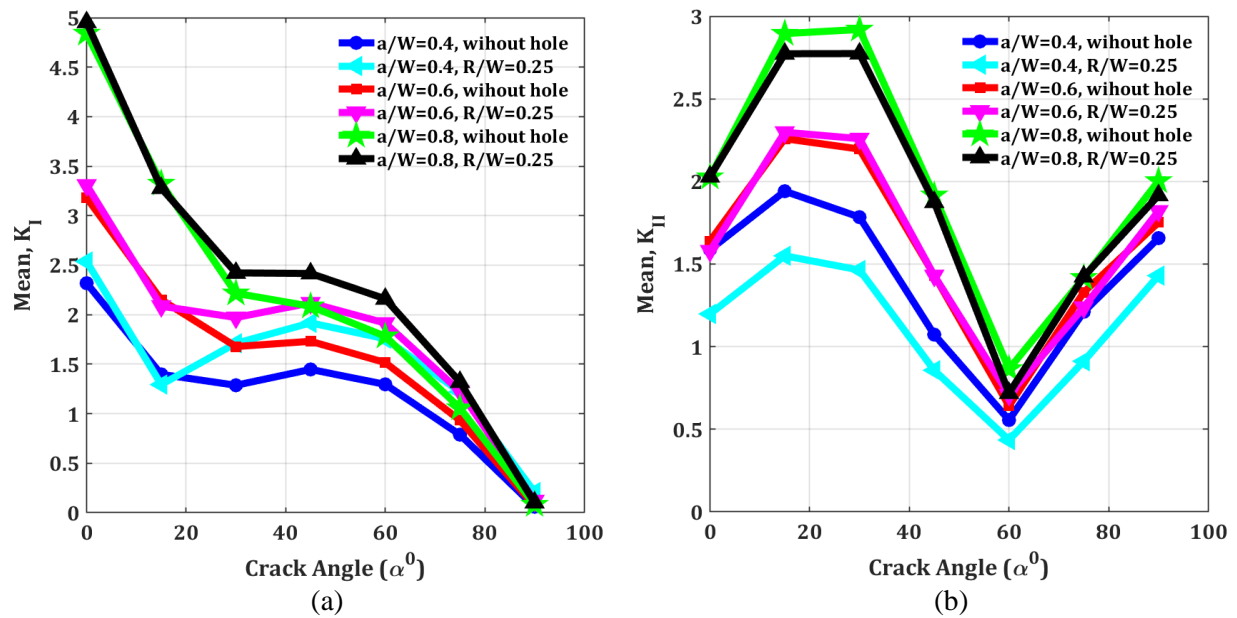


Fig. 6 Comparison of the behavior of the mean and deterministic values of normalized MMSIFs (a) K_I and (b) K_{II} of the plate with a hole and without hole with central cracks of different lengths subjected to combined loading

At the crack angles $\alpha = 0^\circ$ and 90° , the mean values of K_{II} for a plate emanating radial cracks are nearly equal to the deterministic values of $K_{II,det}$ for the cracked plate without hole with the increment in normalized crack length ($a/W = 0.8$). At 60° crack angle, the mean values of K_{II} are nearly equal to the deterministic values of normalized Mode-II SIFs $K_{II,det}$ of an isotropic cracked plate without a hole.

4. Conclusions

The fracture behaviour of the plate with discontinuities subjected to shear and combined loading conditions are much more critical as compared to tensile loading. Hence, proper control of these types of loading will increase the reliability of structures. The input random variables such as normalized crack length, crack angle, and normalized radius of the hole show much influence on the stochastic fracture behavior of the plate with discontinuities. So, the reliability and safety in a structure can be enhanced by controlling the input random variables properly.

Under tensile loadings, the plate is the least critical and sensitive when the geometry (hole emanating cracks) at the centre position and is the most critical and sensitive when the geometry is either side of the central part of the plate. Under shear and combined loadings, the plate is the least critical and sensitive when the geometry is below the central part of the plate and is the most critical and sensitive when the geometry is above the central part of the plate.

References

- [1] Chowdhury, M. S., Song, C., and Gao, W. (2011). Probabilistic fracture mechanics by using Monte Carlo simulation and the scaled boundary finite element method. *Eng. Fract. Mech.* 78, 2369–2389. doi:10.1016/j.engfracmech.2011.05.008.
- [2] Rahman, S., and Chen, G. (2005). Continuum shape sensitivity and reliability analyses of nonlinear cracked structures. *Int. J. Fract.* 131, 189–209. doi:10.1007/s10704-004-3948-6.
- [3] Reddy, R. M., and Rao, B. N. (2008). Stochastic fracture mechanics by fractal finite element method. *Comput. Methods Appl. Mech. Eng.* 198, 459–474. doi:10.1016/j.cma.2008.08.014.
- [4] Chakraborty, A., and Rahman, S. (2008). Stochastic multiscale models for fracture analysis of functionally graded materials. *Eng. Fract. Mech.* 75, 2062–2086. doi:10.1016/j.engfracmech.2007.10.013.
- [5] Chakraborty, A., and Rahman, S. (2009). A parametric study on probabilistic fracture of functionally graded composites by a concurrent multiscale method. *Probabilistic Eng. Mech.* 24, 438–451. doi:10.1016/j.probenmech.2009.01.001.
- [6] Choi, S. K., Canfield, R. A., and Grandhi, R. V. (2007). *Reliability-based structural design*. Canfield R A Springer Verlag London doi:10.1007/978-1-84628-445-8.
- [7] Evangelatos, G. I., and Spanos, P. D. (2011). A collocation approach for spatial discretization of stochastic peridynamic modeling of fracture. *J. Mech. Mater. Struct.* 6, 1171–1195.
- [8] Haldar, A., and Mahadevan, S. (2000). *Probability, Reliability, and Statistical Methods in Engineering Design*. Wiley, New York. doi:10.1061/(ASCE)0733-9445(2001)127:1(101).
- [9] Khasin, V. L. (2014). Stochastic model of crack propagation in brittle heterogeneous materials. *Int. J. Eng. Sci.* 82, 101–123. doi:10.1016/j.ijengsci.2014.04.002.
- [10] Lal, A., and Markad, K. M. (2019). Stochastic mixed mode stress intensity factor of center cracks FGMs plates using XFEM. *Int. J. of Compu. Mat. Sci. and Engg.* 8(3), 1950009. <https://doi.org/10.1142/S204768411950009X>.
- [11] Rahman, S., and Rao, B. N. (2001b). An element-free Galerkin method for probabilistic mechanics and reliability. *Int. J. Solids Struct.* 38, 9313–9330. doi:10.1016/S0020-7683(01)00193-7.
- [12] Paweł, S. (2017). An improved XFEM for the Poisson equation with discontinuous coefficients. *Arch. Mech. Eng.* LXIV, 1–22. doi:10.1515/meceng-2017-0008.

- [13] Pietruszczak, S., and Haghghat, E. (2014). Modeling of Fracture Propagation in Concrete Structures Using a Constitutive Relation with Embedded Discontinuity. *Stud. Geotech. Mech.* XXXVI, 27–33. doi:10.2478/sgem-2014-0033.
- [14] Tian, R., Wen, L., and Wang, L. (2019). Three-dimensional improved XFEM (IXFEM) for static crack problems. *Comput. Methods Appl. Mech. Eng.* 343, 339–367. doi:10.1016/j.cma.2018.08.029.
- [15] Lal, A., and Markad, K. M. (2021). Probabilistic based nonlinear progressive failure analysis of piezoelectric laminated composite shell panels in hygrothermal environment. *J. of Aerospace Engg. (ASCE)*, 34(6). doi.org/10.1061/(ASCE)AS.1943-5525.0001345
- [16] Arregui-Mena, J. D., Margetts, L., and Mummery, P. M. (2016). Practical Application of the Stochastic Finite Element Method. *Arch. Comput. Methods Eng.* 23, 171–190. doi:10.1007/s11831-014-9139-3.
- [17] Lal, A., and Palekar Shailesh, P. (2016). Probabilistic fracture investigation of symmetric angle ply laminated composite plates using displacement correlation method. *Curved Layer. Struct.* 3, 47–62. doi:10.1515/cls-2016-0004.
- [18] Pais, M. (2011a). MATLAB Extended Finite Element (MXFEM) Code v1.2. Available at: www.matthewpais.com.
- [19] Daux, C., Moes, N., Dolbow, J., Sukumar, N., and Belytschko, T. (2000). Arbitrary branched and intersecting cracks with the extended finite element method. *Int. J. Numer. Methods Eng.* 48, 1741–1760.
- [20] Stefanou, G. (2009). The stochastic finite element method: Past, present and future. *Comput. Methods Appl. Mech. Eng.* 198, 1031–1051. doi:10.1016/j.cma.2008.11.007.
- [21] Grasa, J., Bea, J. a., Rodriguez, J. F., and Doblare, M. (2006). The perturbation method and the extended finite element method. An application to fracture mechanics problems. *Fatigue Fract Engng Mater Struct* 29, 581–587. doi:10.1111/j.1460-2695.2006.01028.x.